Hopkinson, C. and Chasmer, L., 2007. Using discrete laser pulse return intensity to model canopy transmittance. *The Photogrammetric Journal of Finland.* Vol. 20. No. 2. pp. 16-26.

# USING DISCRETE LASER PULSE RETURN INTENSITY TO MODEL CANOPY TRANSMITTANCE

Chris Hopkinson [1] and Laura Chasmer [1, 2]

[1] Applied Geomatics Research Group, NSCC Annapolis Valley Campus, Lawrencetown, NS, B0S 1P0, CANADA
[2] Department of Geography, Queen's University, Kingston, ON, K7L 3M6, CANADA

Chris.hopkinson@nscc.ca, lechasme@yahoo.ca

## *ABSTRACT*

*Five comparable airborne lidar datasets were collected over a mixed wood site on five separate occasions throughout a single growing season to capture changing canopy transmittance conditions. Using the small footprint discrete pulse intensity return data, the vertical pulse power distribution was reconstructed for 30 plots each containing 5 digital hemispherical photo (DHP) stations. Canopy gap fraction was calculated for the 150 DHP images collected coincident with the lidar data and used as validation for overhead canopy transmittance. By modifying a Beer-Lambert approach, we relate the ratio of lidar intensity-based ground return power / total return power to the canopy gap fraction. The results are compared to the commonly cited and utilised ground-to-total returns ratio. It is found that for the mixed wood environment studied, a lidar intensity-based power distribution ratio provides a slightly higher coefficient of determination with DHP gap fraction ($r^2$ = 0.92) than does the often used ground-to-total return ratio approach ($r^2$ = 0.86). Moreover, if the intensity power distribution ratio is modified to account for two-way pulse transmission losses within the canopy, the model requires no calibration and provides a 1:1 estimate of the overhead (solar zenith) gap fraction.*

## 1. INTRODUCTION

### 1.1 Rationale

The premise of the study is that the interaction between forest canopy and laser pulses emitted from an airborne lidar (light detection and ranging) mapping system can be considered in some ways analogous to the interaction of direct beam solar radiation with canopy covered environments. We examine the reconstructed vertical pulse power distribution returned from a commercial small footprint discrete pulse airborne laser scanning system and relate properties of the distribution to canopy structural and radiative transfer characteristics. In particular, we compare published gap fraction (P) algorithms to new algorithms that utilize the return intensity information. From the algorithms tested we develop a non-parameterized quasi-physical model of the spatiotemporal variation in canopy gap fraction for a mixed forest landscape. For the purpose of this analysis we make the assumption that overhead gap fraction (P) and overhead transmittance (T) are equivalent.

### 1.2 Leaf Area Index

Leaf area index (LAI) is defined as one half the total leaf area per unit ground surface area ($m^2$ $m^{-2}$) (Chen *et al.* 2006) and is an important parameter for understanding variability in energy, water and carbon fluxes within an ecosystem. LAI and transmittance (T) are key input parameters in many

ecological and hydrological models as they enable the prediction of energy transmission through the canopy to lower layers of biomass or to ground level (e.g. Pomeroy and Dion, 1996). This information is essential in growth (e.g. photosynthesis) and hydrological (e.g. melt and evaporation) process modelling in forested environments. Accurate and consistent LAI measurements are often labour intensive and may also be difficult to collect in remote or difficult to access areas. Measurement methods that cannot differentiate between woody and leafy materials do not measure true LAI, rather they measure the effective leaf area index (Le). The reader is referred to Chen *et al.* (2006) for an in depth look at leaf area index theory, algorithms, and methodologies.

The fraction of incoming photosynthetically active radiation (FIPAR) absorbed by the canopy is the opposite of canopy transmittance and can be calculated from the ratio of downwelling photosynthetically active radiation (PAR) below the canopy to downwelling PAR above the canopy (Gower *et al.* 1999). Chen (1996) states that downwelling PAR above the canopy does not tend to vary spatially during clear conditions, however, downwelling PAR below the canopy varies significantly both in space and time due to canopy structure and openness. FIPAR is closely related to the canopy gap fraction (Gower *et al.* 1999). LE can be estimated from Beer-Lambert's Law (from Gower *et al.* 1999; Leblanc *et al.* 2005):

$$P(q) = e^{-k(q)\Omega(q)Le/\cos(q)} \quad (1)$$

Where P(θ) is gap fraction along zenith angle (θ), k(θ) is the extinction coefficient (fraction of foliage area projected onto a perpendicular plane), and O(θ) is the clumping or non-randomness index (Gower *et al*. 1999; Leblanc *et al*. 2005).

## 1.3 Lidar estimates of P and Le

For every emitted laser pulse, there can be several reflecting surfaces along the travel path. Those backscatter elements that are strong enough to register a distinct amplitude of reflected energy at the sensor are known as 'returns'. For a discrete pulse return system such as the airborne laser terrain mapper (ALTM, Optech Inc., Toronto, Canada), the recorded ranges can be separated into single, first, intermediate and last returns. Single returns are those for which there is only one dominant backscattering surface encountered (e.g. a highway surface). For the ALTM, it is possible to also record two intermediate returns making a total of four possible returns from a single emitted pulse. While there is some slight loss of detection capability between adjacent returns (known as "dead time"), this multiple return capability means that there is a reasonable probability of sampling the dominant canopy and ground elements along the pulse travel path.

Laser pulses that are returned from within the canopy have intercepted enough surface area of foliage to be recorded by the receiving optics within the lidar system. The remaining laser pulse energy from the same emitted pulse continues until it intercepts lower canopy vegetation, low-lying understory and/or the ground surface. Laser pulse returns from the ground surface have inevitably passed through canopy gaps both into and out of the canopy. Increasing numbers of gaps within the canopy will result in gap fractions approaching 100%, whereas fewer gaps within the canopy will result in a gap fraction closer to zero. Lidar estimates of canopy P and Le are often based on the assumption that gap fraction is equivalent to T and from Beer-Lambert's Law:

$$P = T = \frac{I_l}{I_o} = e^{-kLe} \quad (2)$$

Where $I_o$ is open sky light intensity above canopy, $I_l$ is the light intensity after travelling a path length (l) through the canopy and k is the extinction coefficient, which can be approximated to a value of 0.5 in a canopy of spherical leaf distribution (Martens *et al.* 1993) but generally varies between about 0.25 and 0.75 for natural needle- and broad-leaf canopies (Jarvis and Leverenz, 1983). The main geometric difference between the canopy interaction of solar and airborne lidar laser pulse radiation is that solar radiation can be incident at all zenith angles if its temporal distribution is considered while laser pulses are typically incident only at overhead ($\theta = 0$ to 30 degrees) angles. Therefore, any direct lidar estimate of P will be for overhead gap fraction only and for a path length close to the height of the canopy. However, by assuming randomly dispersed foliage elements and an isotropic canopy radiation environment (i.e. equal transmittance in all directions) it is possible to derive a first approximation of Le as a function of the overhead gap fraction:

$$Le = -\frac{Ln(P)}{k} \quad (3)$$

Numerous studies have examined the use of lidar for obtaining P, Le, FIPAR and k from lidar (e.g. Magnussen and Boudewyn, 1998; Parker *et al*. 2001; Todd *et al*. 2003; Morsdorf *et al*. 2006; Thomas *et al*. 2006). In particular, Solberg *et al*. (2006) used a similar approach to that illustrated in equation (3) and assumed that P could be approximated by the ratio of below canopy returns to total returns. A similar but simpler approach was taken by Barilotti *et al.* (2006) where the same ratio was found to linearly correlate with LAI. The assumptions of these two studies were corroborated by Riaño *et al*. (2004) and Morsdorf *et al.* (2006) where the ratio of lidar canopy returns to all returns was found to be a reasonable indicator of the inverse of gap fraction; i.e. fractional canopy cover (and even LAI as observed by Magnussen and Boudewyn (1998)). Morsdorf *et al.* (2006) compared canopy lidar fractional cover estimates with field-based DHP fractional cover and found the best correlation was returned when using first return data only ($r^2$ = 0.73). A method for estimating LAI that utilised laser profiling techniques was presented by Kusakabe *et al.* (2000), where field plot measures of LAI were compared to the cross-sectional area contained within the lidar surface profile across the plots. The rationale underlying this approach was that LAI would increase with tree height and stem density, and both of these physical attributes would act to increase the cross sectional area of a lidar profile across a plot.

Common to the studies mentioned is that they all used laser pulse return height attributes but not the intensity. Intensity is generally recorded as a scaled index of the reflected pulse energy amplitude for each range measured by the lidar sensor (Optech Inc. pers. comm.). This information has implicitly been used in estimates of canopy gap fraction in the full waveform lidar literature where the strength of the returned signal from within or below the canopy is considered to be directly related to the transmissivity of the canopy. For example, in Lefsky *et al.* (1999), it was suggested that canopy fractional cover can be estimated as a function of the ratio of the power reflected from the ground surface divided by the total returned power of the entire waveform. It was further suggested that this power ratio needed to be adjusted as a function of different reflectance properties at ground and canopy level.

For airborne laser pulses encountering and returning from a forested canopy at near-nadir scan angles, we cannot easily estimate the incident pulse intensity as it enters the canopy; neither can we

measure the transmitted intensity after it has passed through the canopy. However, by considering the total reflected energy from the canopy to ground profile as being some proportion of the total available laser pulse intensity, and the reflected energy from ground level as a similar proportion of the transmitted pulse energy, we have a means of estimating total canopy transmissivity at near-nadir angles. Further we can assume that atmospheric transmission losses for all outgoing and returning laser pulses are similar and small in magnitude relative to canopy losses, and therefore can be ignored. By building on the work of Lefsky *et al.* (1999), Parker *et al.* (2001) and adapting equation (2), a general pulse return power relationship can be described for gap fraction by:

$$P = f\frac{\sum I_b}{\sum I_t} \tag{4}$$

Where $SI_b$ is below canopy power (the sum of all ground return intensity) and $SI_t$ is the total power (sum of all intensity) for the entire canopy to ground profile. However, this model does not explicitly account for potentially different probabilities associated with receiving a return signal from the ground or canopy level; i.e. the ground and lower level canopy return signals might incur two-way transmission losses due to travelling both into and out of the canopy, while those return signals at the outer envelope of the canopy do not incur any canopy transmission losses. For discrete return data, it is fair to assume that first and single returns generally have not incurred any appreciable transmission loss prior to being reflected back towards the sensor. However, intermediate or last returns are, by definition, a reflected component of the residual energy left over after a previous return was reflected from a surface encountered earlier in the travel path of the emitted pulse. From Beer-Lambert's Law and assuming uniform transmission losses per unit path length travelled, it is possible that a below canopy (ground level) return incurs a similar proportion of transmission loss during its exit from the canopy as it did on the way into the canopy. This leads to a variation of equation (4) such that for those secondary returns from within or below the canopy:

$$P = f\sqrt{\frac{\sum I_b}{\sum I_t}} \tag{5}$$

The analysis presented in this paper builds on the previous research in a number of ways: 1) to sample a range of canopy Le and light conditions, data are collected from multiple sites across an entire growing season; 2) the previously published discrete return ratio method of computing gap fraction is compared to plot-level field DHP data; and 3) new discrete return gap fraction methods are developed and tested based on equations (4) and (5) utilizing the pulse intensity information as an indicator of transmission losses within the canopy.

## 2. STUDY AREA

The study was conducted over a flat to rolling valley site (< 50 m total elevation variation) near Nictaux in the Acadian forest ecozone of Nova Scotia (Figure 1). The study area was less than 1 km wide by approximately 2 km long and comprised a number of common land cover types for this region: predominantly Acadian mixed woodland (mostly yellow birch - *Betula alleghaniensis* Britton, with some mixed pine - *Pinus* and mixed spruce - *Picea* trees). The site is the subject of ongoing lidar and agro-forestry experiments, for which supplemental ground control, plot mensuration and DHP data exist (Hopkinson *et al.* 2006; Hopkinson, 2007).

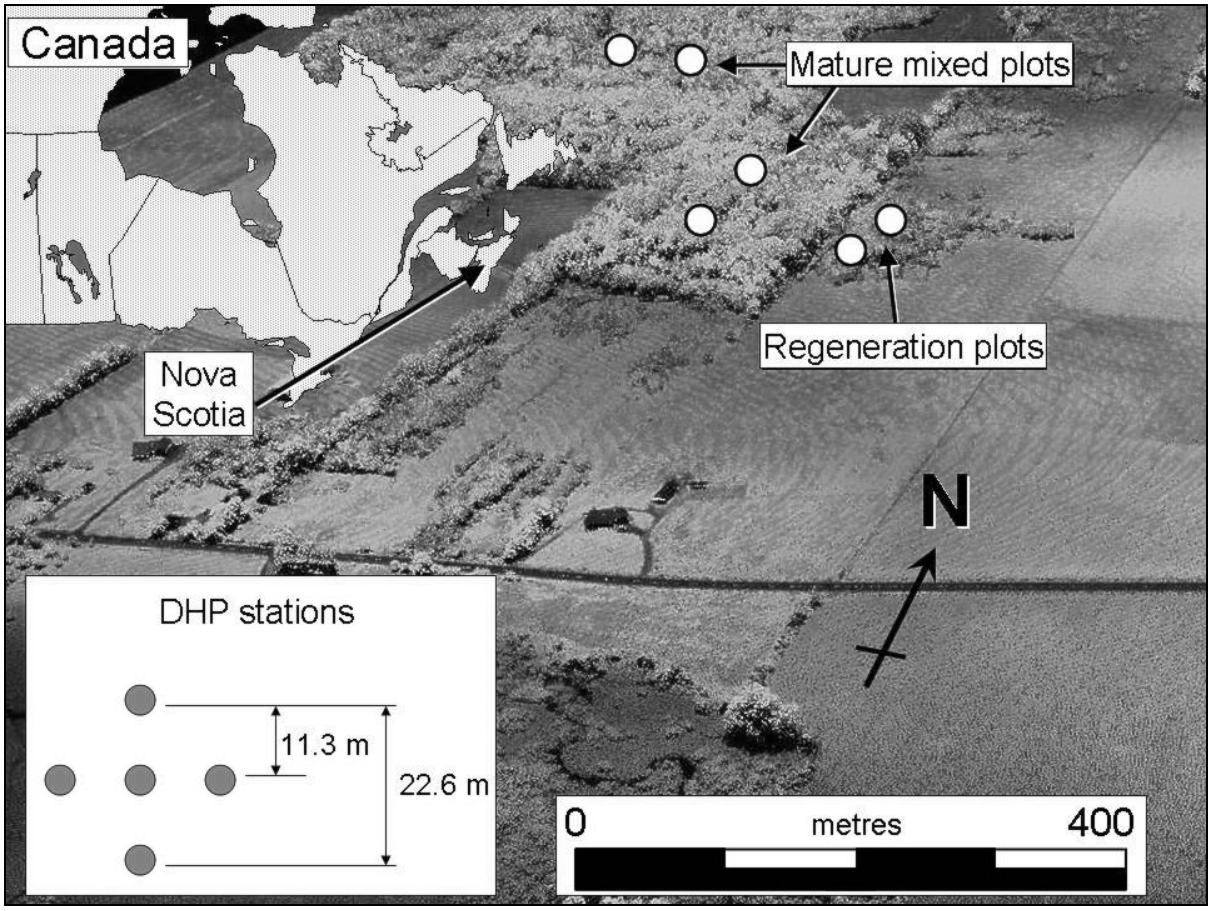

Figure 1. Oblique 3D laser intensity image of study area illustrating sample plot locations. Study site location in Canada (top left) and DHP station set up in each plot (inset bottom left).

## 3. METHODS

### 3.1 DHP data collection and analysis

Effective leaf area index (Le) and canopy gap fraction (P) data were collected and analysed using the digital hemispherical photography (DHP) procedures outlined in Leblanc, *et al*. (2005). DHP data collection took place on five separate occasions: April 8th, May 12th, May 28th, August 18th and October 8th. The first collection was during early spring leaf off conditions, while the second was at the commencement of leaf flush. The May 28th dataset was at intermediate seasonal leaf area levels, while August 18th was close to maximum leaf area. The final dataset was collected during the autumn senescence and leaf drop period. These five datasets, therefore, captured a good temporal representation of the seasonal growth cycle, and variable leaf area and transmittance conditions (Figures 2 and 3).

Six Acadian mixed wood plots were established and the centre of each located using Leica SR530 global positioning system (GPS) receivers differentially corrected to the same base coordinate that was used for the airborne lidar survey. (In total we set up nine plots but the data for plots 5, 6 and 7 were not collected). Each of the six plots contained five photograph stations: one at the plot centre and one at an 11.3 m radius out from the centre at each of the four cardinal compass directions (Figure 1). Each station (30 in total) was marked with a stake to allow each location to be revisited. The camera was always set up level at 1.3 m above ground level to ensure consistent data collection. In total, 150 individual photographs were collected during the growing season of 2006.

All photographs were collected late in the evening on each day, immediately prior to dusk, to minimize direct sunlight and ensure even background sky illumination conditions. Photographs were collected using a Nikon Coolpix E8800 camera with a $180^{o}$ fisheye (FC-E9) lens set at 8 mega pixels with an exposure setting one f stop smaller than the automatic exposure reading to slightly under-expose the image and increase contrast between vegetation and sky. Each photograph was processed using DHP version 1.6.1 software (S. Leblanc, Canada Centre for Remote Sensing provided to L. Chasmer through the Fluxnet-Canada Research Network). Chen *et al*. (2006) note that effective LAI estimates based on DHP procedures tend to correlate well ($r^2 \sim 0.86$) and provide values within 25% of other widely accepted effective LAI measurement procedures. Our own tests of repeatability conducted over 5 sites two days apart demonstrated a mean Le difference of 1.3%, a maximum individual plot difference of 5.9% and a coefficient of determination ($r^2$) across all plots of 0.68. These observations provided confidence that the seasonal Le values obtained using the DHP procedure outlined were repeatable and consistent.

## 3.2 Lidar data collection and preparation

The lidar sensor used was an Optech Incorporated (Toronto, Ontario) airborne laser terrain mapper (ALTM) 3100 owned by the Applied Geomatics Research Group (AGRG) operating at a wavelength of 1064 nm. All data were collected and processed by the authors. Five datasets were collected in 2006 coincident (within two days) of the DHP field data collections. All airborne lidar acquisitions were collected during dry conditions and using the same sensor and platform configuration to control for sensor effects (see Hopkinson, 2007). The surveys were flown at 1000 m a.g.l., 70 kHz pulse repetition frequency, peak pulse power of 7.2 kW, 0.3 mRad beam divergence (1/e) producing a footprint diameter on the ground of approximately 0.3 m, ±15 degree from nadir scan angle (30 degree field of view), 50% swath overlap with roll compensation to keep survey swaths uniform. These settings provided a sampling density of approximately 3 points per $m^2$ and ensured that every point on the ground was observed from two directions at a mean viewing angle of 7.5 degrees.

The airborne GPS trajectories were differentially corrected to the AGRG GPS base station receiver less than 5 km from the centre of the survey site. Raw lidar ranges and scan angles were integrated with aircraft trajectory and orientation data using *PosPAC* (Applanix, Toronto) and *REALM* (Optech, Toronto) software tools. The outputs from these procedures were a series of flight line data files containing xyzi (easting, northing, elevation, intensity) information for each laser pulse return collected. All intensity data were normalised to a range of 1000 m to mitigate against geometric variations in intensity due to scan angle, terrain relief and aircraft altitude variation (see Hopkinson, 2007).

Following lidar point position computation, the xyzi data files were imported into the *Terrascan* (Terrasolid, Finland) software package for plot subsetting and to separate canopy and below canopy returns. The data acquired for the leaf-off April $8^{th}$ data collection were classified using the Terrascan morphological ground classification filter to provide a digital elevation model (DEM) to which all datasets could be normalised. After normalization, all elevations for all datasets were relative to the same ground level datum; i.e. possessed heights ranging from 0 m to approximately 25 m. This allowed all returns to be divided into canopy and below canopy returns using a height threshold of 1.3 m to coincide with the height of the DHP field data.

For each of the 30 DHP stations, all laser pulse return data were extracted within a circular radius of 11.3 m. This radius was chosen as it was: a) consistent with field mensuration practices; b) was the distance between adjacent photo stations and thus provided complete plot lidar coverage; and c) was close to the optimal radius of approximately 15 m observed in Mosdorf *et al.* (2006). In addition to the canopy and below canopy classes, the return data were further subdivided into four sub-classes related to the order of the return itself; i.e. single, first, intermediate and last returns. For the canopy class, it is possible for a return to belong to any one of the four sub classes (provided the canopy is deep enough), however, ground returns can only belong to either the last or single return sub class. This subdivision was carried out as the return number and its position in the sequence indicates whether or not the pulse has been split and therefore potentially susceptible to energy transmission losses on its way into and out of the canopy.

### 3.3 Lidar gap fraction analysis

Gap fraction estimates were extracted for each of the individual DHP stations and related to plot-level lidar data derived using four methods. The modelled lidar gap fraction estimates were compared with the DHP calculations from both the single overhead annulus ring (0 - 10 degrees) and nine ring hemispherical (0 – 80 degree) data. The first method used the ratio of ground level (below canopy) returns to total returns and was known as the pulse return ratio method ($P_{rr}$). This method is similar to that of Solberg *et al.* (2006) and has parallels to the fractional cover methods presented by Riaño *et al.* (2004) and Morsdorf *et al.* (2006). Further, laser pulse return power ratio methods were generated using return intensity data. Three variations were tested: 1) The simple pulse intensity power ratio is based on equation (4) with no modification; i.e. Gap fraction ($P_{ipr}$) is estimated as the ratio of the sum of all ground level return intensities divided by the sum of total return intensity; 2) Based on the work of Lefsky (1999), the pulse intensity power ratio method was modified slightly by assuming ground level surfaces were half as reflective as canopy foliage and so the energy returned from these surfaces was amplified by a factor of two:

$$P_{ipv} = \frac{2 \times \sum I_{Ground}}{\sum I_{Canopy} + \left(2 \times \sum I_{Ground}\right)} \tag{6}$$

and 3) the square root power ratio ($P_{sqr}$) is modified from equation (5) to account for a potential two-way transmission loss of pulse energy for intermediate or last returns as follows (all reflecting surfaces were assumed to have an equal reflectance probability):

$$P_{sqr} = \frac{\left(\frac{\sum I_{GroundSingle}}{\sum I_{Total}}\right) + \sqrt{\frac{\sum I_{GroundLast}}{\sum I_{Total}}}}{\left(\frac{\sum I_{First} + \sum I_{Single}}{\sum I_{Total}}\right) + \sqrt{\frac{\sum I_{Intermediate} + \sum I_{Last}}{\sum I_{Total}}}} \tag{7}$$

Where each subscript refers to the class and/or sub-class of pulse return. In this model, first and single returns incur no reverse transmission loss through canopy and so are not square rooted, while intermediate and last returns could potentially lose similar proportions of energy due to interception on both incoming and outgoing transmission; i.e. a power function loss.

## 4. RESULTS AND DISCUSSION

The seasonal variation in DHP gap fraction ($P_{DHP}$) is clearly visible in Figure 2. The mean overhead (0 to 10 degrees zenith) and hemispherical (0 to 80 degrees zenith ) $P_{DHP}$ statistics, lidar ground-to-total return ratio ($P_{rr}$), the simple intensity power ratio ($P_{ipr}$) and the square root intensity power ratio ($P_{sqr}$), along with the coefficients of determination ($r^2$) are presented in Table 1. All results illustrate high correlations with gap fraction (or fractional cover). While there are high and very similar correlations for all three lidar gap fraction methods, we see that the simple intensity power distribution ratio provides the most robust model. It should be noted, however, that there is no statistical difference in the explanatory power of the models tested; i.e. any one of the models is a reliable indicator of gap fraction and if another dataset or environment were investigated, the ranking of the models might change.

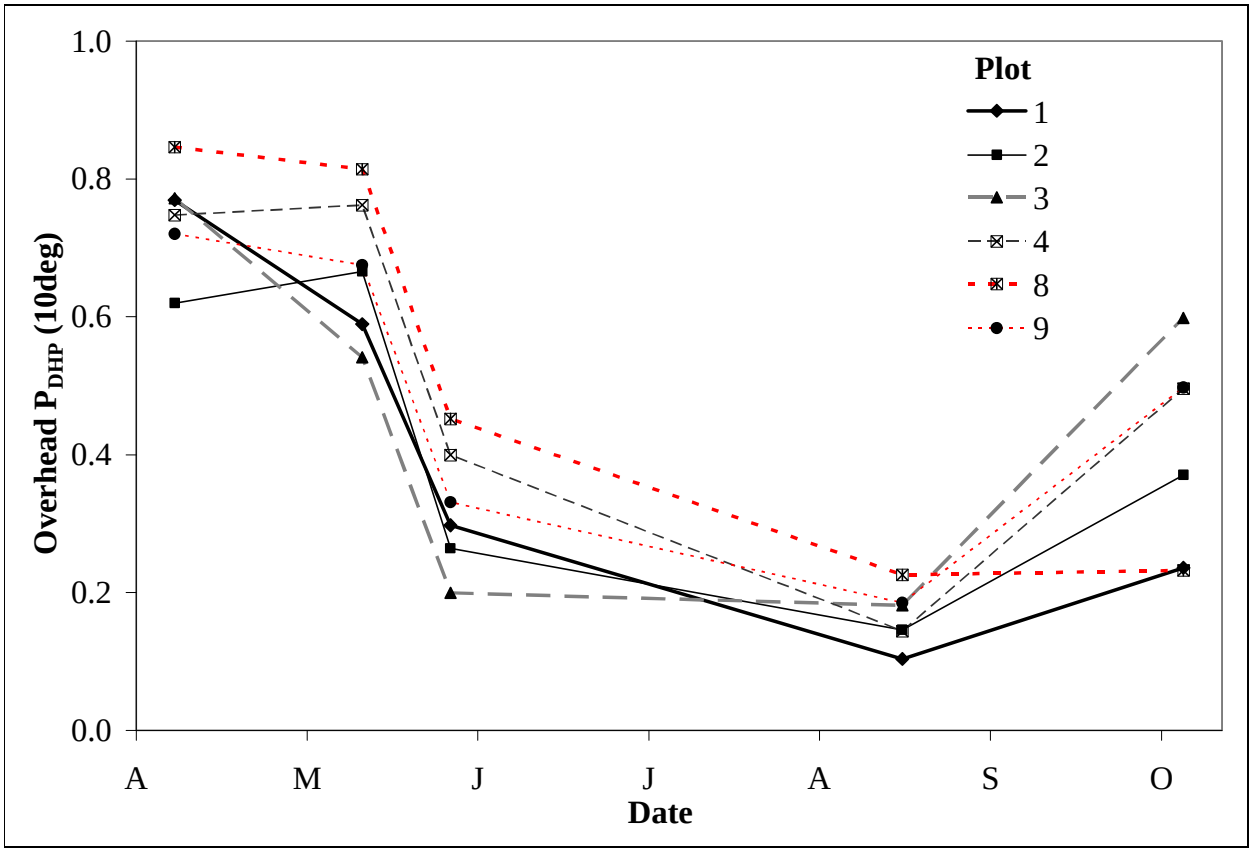


Figure 2. Plot-level seasonal DHP overhead gap fraction.

| | Summary | | Intercept | | Slope | | $r^2$ | |
|---|---|---|---|---|---|---|---|---|
| | Mean | SD | $P_{DHP}$ 10 deg | $P_{DHP}$ 80 deg | $P_{DHP}$ 10 deg | $P_{DHP}$ 80 deg | $P_{DHP}$ 10 deg | $P_{DHP}$ 80 deg |
| $P_{DHP}$ (10 degree) | 0.46 | 0.24 | | 0.04 | | 0.70 | | 0.93 |
| $P_{DHP}$ (80 degree) | 0.36 | 0.17 | -0.02 | | 1.32 | | 0.93 | |
| Ground return ratio ($P_{rr}$) | 0.38 | 0.18 | 0.02 | 0.03 | 1.17 | 0.89 | 0.80 | 0.86 |
| Intensity power ratio ($P_{ipr}$) | 0.43 | 0.31 | 0.15 | 0.13 | 0.72 | 0.53 | 0.90 | 0.92 |
| Intensity ratio with variable reflectance ($P_{ipv}$) | 0.53 | 0.32 | 0.08 | 0.08 | 0.72 | 0.53 | 0.89 | 0.92 |
| Square root power ratio ($P_{sqr}$) | 0.46 | 0.25 | 0.05 | 0.06 | 0.90 | 0.67 | 0.87 | 0.91 |

Table 1. Gap fraction summary statistics and regression results (n = 150)

The $r^2$ values for the DHP 9 ring (0 to 80 degree) hemispheric gap fraction results are consistently higher than those for the single overhead annulus ring (0 to 10 degree) due to the larger area sampled and subsequent increased stability in the data (Table 1). For the overhead DHP gap fraction, the small field of view (radius of ~ 3.5 m at a canopy height of 20 m), leads to an increased likelihood of localised variations in canopy gaps that are not representative of the overall canopy conditions. Regarding the absolute magnitude of P, we see that the intensity-based methods produce values (0.43, 0.53 and 0.46 for $P_{ipr}$, $P_{ipv}$ and $P_{sqr}$, respectively) that are all within 15% of the overhead DHP value (0.46), while the pulse return ratio value (0.38) under-estimates by 17%. The square root intensity-based method ($P_{sqr}$) provided the closest estimate both in magnitude and in variance (expressed as the standard deviation), despite a non significant lower explanation of the variance ($r^2 = 0.87$) than for $P_{ipr}$ ($r^2 = 0.90$) or $P_{ipv}$ ($r^2 = 0.89$). Apart from the simple intensity power ratio ($P_{ipr}$), all other lidar gap fraction method intercepts were within 0.1 (or 10%) of 0. However, both simple intensity power ratio methods ($P_{ipr}$ and $P_{ipv}$) plots displayed slopes that deviated greater than 25% from a 1:1 relationship with the overhead DHP gap fraction. It is worth noting that attempting to compensate for the generally lower surface reflectance at ground level by amplifying the intensity of below canopy returns ($P_{ipv}$) provided slightly poorer overall results (Table 1) than the simple ground / canopy intensity return power ratio ($P_{ipr}$). The ground return ratio ($P_{rr}$) method was closer with a slope of 1.17 but of all methods tested, the square root intensity power ratio ($P_{sqr}$) was the closest being within 10% at 0.9.

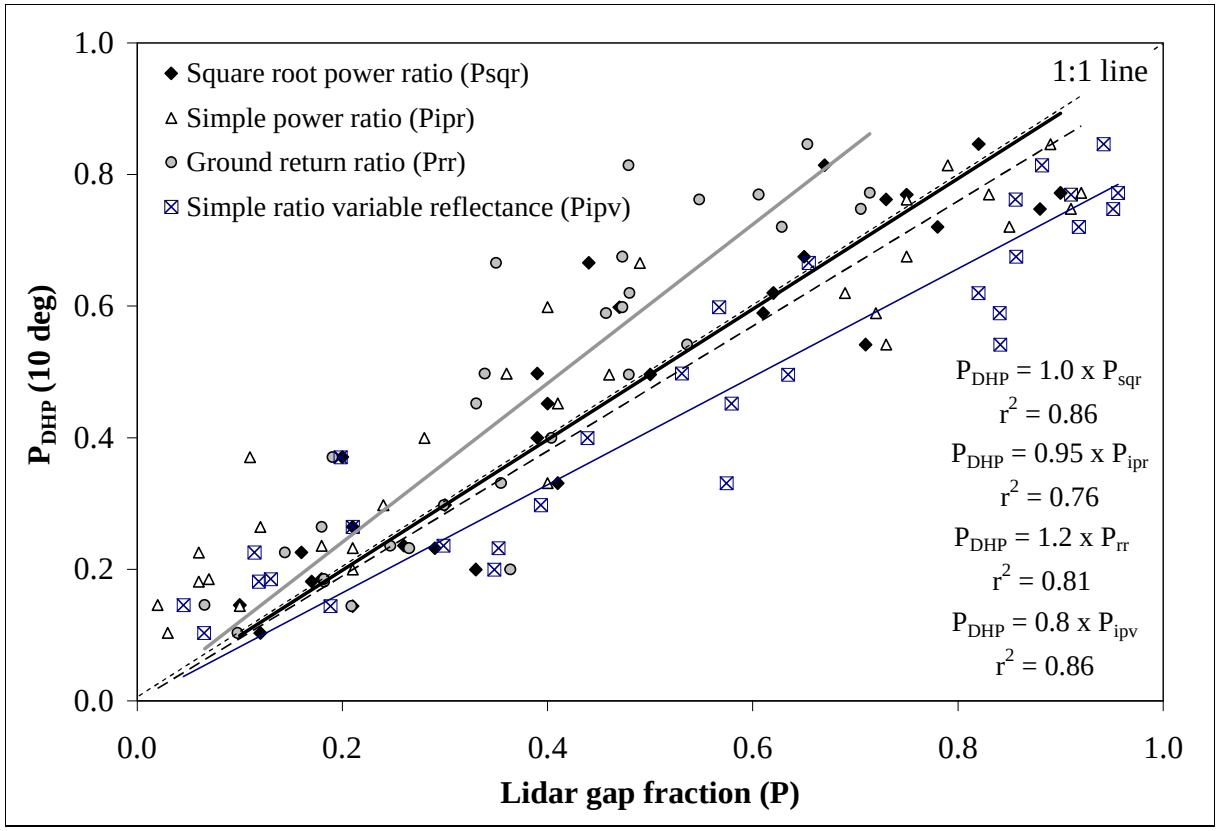


Figure 3. DHP overhead gap fraction ($P_{DHP}$) with lidar gap fraction. All regression lines are forced through the origin.

The high correlation and close match in absolute values is further illustrated in Figure 3, where the regression lines are forced through the origin. We clearly see a 1:1 relationship between $P_{DHP}$ and $P_{sqr}$, while all other methods deviate from unity between 5% and 20%. Further, by forcing the

regression line through the origin, the explanation of variance is altered and $P_{sqr}$ now displays the highest $r^2$ at 0.86. This suggests that by applying a two-way Beer-Lambert Law transmission loss to the intermediate and last return intensity values, we are more accurately recreating the laser pulse power distribution. These results also clearly demonstrate that by including the intensity data, we achieve both a better correlation with, and more accurate estimates of, canopy gap fraction. Of most significance here is that the lidar intensity based estimate of gap fraction appears to require no calibration.

## 5. CONCLUSION

While lidar ground-to-total return ratios have been demonstrated in the published literature to show strong correlation to canopy gap fraction and fractional coverage, it is shown here that for the mixed wood environment studied, the model can be improved slightly ($r^2$ increase from 0.86 to 0.92) by considering the lidar power distribution ratio as reconstructed from the laser pulse intensity data. Moreover, if the intensity power distribution is modified to account for potential secondary return two-way pulse transmission losses within the canopy, the resultant gap fraction model requires no calibration and provides a 1:1 direct estimate of overhead gap fraction. This is an improvement over the ground-to-total pulse return ratio where it was found that despite a good correlation with DHP gap fraction, the actual value predicted was under-estimated by approximately 17%. The implications of these observations are that: a) canopy transmissivity in overhead zenith directions can be directly quantified from lidar data without the need for ground calibration; and b) if the canopy extinction coefficient is *a priori* known or can be estimated from look up tables, the effective leaf area index can also be mapped directly from the lidar point cloud intensity data.

### 5.1 References


Barilotti A., Turco S., Alberti G. 2006. *LAI determination in forestry ecosystems by LiDAR data analysis*. Workshop on 3D Remote Sensing in Forestry, 14-15/02/2006, BOKU Vienna.

Chen, J.M. 1996. Optically-based methods for measuring seasonal variation in leaf area index of boreal conifer forests. *Agric. Forest Meteorol*. 80: 135-163.

Chen, J.M., Govind, A., Sonnentag, O., Zhang, Y., Barr, A., Amiro, B. 2006. Leaf area index measurements at Fluxnet-Canada forest sites. *Agric. Forest Meteorology*, 140:257-268.

Gower, S.T., Kucharik, C. J., Norman, J.M. 1999. Direct and indirect estimation of leaf area index, $f_{APAR}$, and net primary production of terrestrial ecosystems. *Remote Sensing of Environment*, 70:29-51.

Hopkinson, C. 2007. The influence of flying altitude and beam divergence on canopy penetration and laser pulse return distribution characteristics. *Canadian Jnl of Remote Sensing*, 33(4): 312-324.

Hopkinson, C., Chasmer, L., Lim, K., Treitz, P., Creed. I. 2006. Towards a universal lidar canopy height indicator. *Canadian Jnl of Remote Sensing*, 32(2): 139-152.

Jarvis P.G., Leverenz J.W. 1983. Productivity of temperate, deciduous and evergreen forests. In: Lange OL, Nobel PS, Osmond CB, Zeigler H, eds. Physiological plant ecology IV. Ecosystem processes: mineral cycling productivity and man's influence. *Encyclopedia of plant physiology*, Vol. 12D. Berlin: Springer Verlag, 233-80.

Kusakabe, T., Tsuzuki, H., Hughes, G., Sweda, T. 2000. Extensive forest leaf area survey aiming at detection of vegetation change in subarctic-boreal zone. *Polar Biosci*., 13: 133-146.

Leblanc, S.G., Chen, J.M., Fernandes, R., Deering, D., Conley, A. 2005. Methodology comparison for canopy structure parameters extraction from digital hemispherical photography in boreal forests. *Agric. and Forest Meteorology.* 129:187-207.

Lefsky, M.A., Cohen, W.B., Acker, S.A., Parker, G.G., Spies, T.A., Harding. D. 1999. Lidar Remote Sensing of the Canopy Structure and Biophysical Properties of Douglas-Fir Western Hemlock Forests. *Remote Sens. Environ.*, 70: 339-361.

Magnussen, S., Boudewyn. P. 1998. Derivations of stand heights from airborne laser scanner data with canopy-based quantile estimators. *Can. Jnl of Forest Research* 28: 1016-1031.

Martens, S.N. Ustin, S.L. Rousseau, R.A. 1993. Estimation of tree canopy leaf area index by gap fraction analysis. *For. Ecol. Manage.* 61: 91-108.

Morsdorf, F., Kotz, B., Meier, E., Itten, K.I., Allgower. B. 2006. Estimation of LAI and fractional cover from small footprint airborne laser scanning data based on gap fraction. *Remote Sensing of Environment*, 104(1):50-61.

Parker, G.G., Lefsky, M.A., Harding. D.J. 2001. Light transmittance in forest canopies determined using airborne laser altimetry and in-canopy quantum measurements. *Remote Sensing of Environment*, 76: 298-309.

Pomeroy, J.W., Dion, K., 1996. Winter radiation extinction and reflection in a boreal pine canopy: measurements and modelling. *Hydrological processes*. 10: 1591-1608.

Riaño, D., Valladares, F., Condes, S., Chuvieco. E., 2004. Estimation of leaf area index and covered ground from airborne laser scanner (Lidar) in two contrasting forests. *Agricultural and Forest Meteorology*, 124(3-4):269-275.

Solberg, S., Næsset E., Hanssen, K.H., Christiansen, E. 2006. Mapping defoliation during a severe insect attack on Scots pine using airborne laser scanning. *Remote Sensing of Environment,* 102: 364-376.

Todd, K.W., Csillag, F., Atkinson. P.M. 2003 Three-dimensional mapping of light transmittance and foliage distribution using lidar. *Canadian Journal of Remote Sensing*, 29(5):544-555.

Thomas, V; Treitz, P; McCaughey, J H.; Morrison, I. 2006. Mapping stand-level forest biophysical variables for a mixedwood boreal forest using lidar: an examination of scanning density. *Can. Jnl of Forest Research*, 36(1): 34-47.

## 5.2 Acknowledgements

The Canada Foundation for Innovation (CFI) and the Natural Sciences and Engineering Research Council (NSERC) is gratefully acknowledged for supporting this research. The AGRG post-graduate interns, Chris Beasy, Tristan Goulden, Peter Horne, and Kevin Garroway are thanked for their assistance with field data collection.